Canadian Geotechnical Journal

Submitted: 20 April 2023; **Accepted:** 22 September 2023

Stability analysis of heterogeneous infinite slopes under rainfall-infiltration by means of an improved Green-Ampt model

Shui-Hua Jiang

School of Infrastructure Engineering, Nanchang University, 999 Xuefu Road, Nanchang 330031, China.

E-mail: sjiangaa@ncu.edu.cn

Xian Liu*

School of Civil Engineering, Sun Yat-Sen University, Zhuhai 519082, China

School of Infrastructure Engineering, Nanchang University, 999 Xuefu Road, Nanchang 330031, China

E-mail: liux597@mail2.sysu.edu.cn

Guotao Ma*

School of Engineering, University of Warwick, Coventry, CV4 7AL, UK

E-mail: derek.ma.1@warwick.ac.uk

Mohammad Rezania

School of Engineering, University of Warwick, Coventry, CV4 7AL, UK

E-mail: m.rezania@warwick.ac.uk

*Corresponding author

E-mail: liux597@mail2.sysu.edu.cn; derek.ma.1@warwick.ac.uk

6900 words, 12 figures and 5 tables

ABSTRACT

Rainfall infiltration analysis has a great significance to the mitigation and risk assessment of rainfall-induced landslides. The original Green-Ampt (GA) model ignored the fact that a transitional layer exists in infiltration regions of soils under the rainfall permeation, therefore it cannot effectively analyze the rainfall-infiltrated heterogeneous slope considering the spatial variability of saturated hydraulic conductivity (k_s). In this paper, an improved GA model is proposed for the rainfall-infiltration analysis of heterogeneous slopes. Four common slope cases are investigated to validate the effectiveness of the proposed model. An infinite slope model is taken as an illustrative example to investigate the distributions of volumetric water content and slope stability under the rainfall infiltration. The results show that the distributions of volumetric water content and factors of safety (*Fs*) obtained from the proposed model are in very good agreement with the numerical results of Richards equation. In contrast, the modified GA model obtains biased distributions of volumetric water content and smaller *Fs* for the same cases. The results show that the proposed GA model can accurately identify the location of critical slip surface of the slope, and as such it provides an efficient method for risk control analysis of slopes susceptible to landslide.

Keywords: Infinite slope; Slope stability; Rainfall infiltration; Improved Green-Ampt model; Spatial variability

1 Introduction

Over 90% of slope instability and landslide cases are associated with rainfall (Ko et al., 2018; Yang et al. 2022), and rainfall infiltration has been recognized as one of the most dominant triggers of landslide disasters worldwide (e.g., Ng and Shi, 1998; Cho and Lee, 2002; Ma et al. 2018). During the rainfall infiltration, there is an increase of water content of soil that leads to a reduction of matric suction, which results in the increase of the sliding forces which eventually induces slope instability and landslide. It has been reported that the number of landslides tends to increase with the increasing heavy rainfall events due to the global climate changing trend (Chang et al. 2021; He et al., 2023). To predict and mitigate for potential damages and fatalities, development of effective stability model for slopes under rainfall infiltration is essential.

To date, considerable efforts have been made to tackle rainfall infiltration problem, the commonly used methods primarily fall into the following two categories: (1) numerical analysis methods based on the Richards equation and continuum mechanics (Ng and Pang, 2000; Zhang et al., 2004; Phoon et al., 2007; Simunek et al., 2013; Zhan et al., 2023); (2) analytical methods (Zhang and Ng, 2004) based on physical infiltration models, e.g., Green-Ampt (GA) infiltration model (Green and Ampt, 1911), Smith model (Smith et al., 1993), and Philip model (Philip, 1957), etc. Since numerical methods require iterative calculation procedure to solve governing equations of rainfall infiltration, the corresponding computing process is particularly tedious and time-consuming (Phoon et al., 2007). On the other hand, analytical methods with notable computational efficiency and transparent physical bases, such as the GA infiltration model, have been significantly developed and employed to analyze the water infiltration process in soils and

associated slope stability. The GA model, the widely used analytical method, had been developed to deal with different infiltration boundaries caused by the variability of saturated hydraulic conductivity (k_s) (e.g., Chen and Young, 2006; Dou et al., 2014; Jiang et al., 2020). Additionally, the distribution of moisture content and depth of wetting front in the process of rainfall infiltration can be effectively determined by the GA model, which has been successfully applied in several slope stability studies (Cho and Lee, 2002; Muntohar and Liao, 2009; Yao et al., 2019) and reliability analyses (Dou et al., 2014; Zhang et al., 2014a; Jiang et al., 2020; Yu et al., 2022). For instance, Liu et al. (2021) proposed a new GA model for describing the two-stage infiltration in slopes based on fractional derivatives. Dolojan et al. (2021) adopted the GA model for analyzing shallow slope failures induced by rainfall infiltration. However, although these works greatly expanded the applicability of the GA model, they ignored the existence of unsaturated transitional layer in the wetting soil zone. Numerous studies have demonstrated that the soil between the wetting front and the infiltration surface is not fully saturated, there is at least one transitional layer between the saturated and the natural zone. Additionally, divergent water content at different depths in the transitional layer can be found (Wang et al, 2003; Peng et al, 2012). According to the mathematical function proposed by Zhang et al. (2014b), with assumption of soil stratification the relationship between the rainfall duration and the wetting front depth of the GA model can be found. Based on the stratified GA model, Hu et al. (2019) analyzed the rainfall infiltration process of unsaturated loess under the effect of water ponding. Yao et al. (2019) set the thickness of saturated layer

and unsaturated layer to be 50% of the depth of the infiltration zone and conducted stability analyses of an infinitely long slope and a landslide case.

The randomness and heterogeneity of geomaterials are widely admitted, as the consequences of geological activities such as sedimentation (e.g., Phoon and Kulhawy, 1999; Jiang et al., 2014; Masoudian et al., 2019; Ma et al., 2022a, 2022b, 2022c; Liu et al., 2023). In particular, the k_s of soils in slopes usually exists significant spatial variability. The k_s is not a large value either a small value but varies with locations. It has been proved that the process of rainwater infiltration in the slope is largely dependent on the k_s of soil constituting the slope. The spatial variability of k_s significantly influences the matric suction as well as other hydraulic parameters and consequently the slope stability (Ng et al., 2022; Li et al., 2023). A large k_s implies that the rainwater can easily infiltrate into the slope base in short time; whereas, a low k_s means that the rainwater is hard to permeate into the slope and thus has little effect on the slope stability. Ignoring the spatial variability of k_s would lead to the miscalculation of slope failure probability (Santoso et al., 2011; Cho et al., 2014; Dou et al., 2014; Masoudian et al., 2019; Liao et al., 2021). Therefore, it is essential to reasonably characterize the influence of its spatial variability when conducting the rainfall infiltration analysis (Cho 2014; Jiang et al., 2014). The GA model has been developed to consider the natural variability of k_s (Dou et al., 2014), however, there is currently no GA model that is capable to investigate slope stability considering the spatial variability of k_s.

To address the above issues, this paper aims to propose a new GA model that can accurately investigate the evolving water distribution under rainfall infiltration and analyse its influence on heterogeneous slope stability. The paper is organized as follows. In section 2,

the classic GA model and the proposed improved GA model are introduced. In section 3, the implementation procedure for stability analysis of a spatially varying soil slope based on the improved GA model is presented. In section 4, four common cases are conducted to validate the effectiveness of the improved GA model. Finally, brief conclusions are drawn in Section 5.

2 Methodology

2.1 Classic Green-Ampt model

In 1911, the original GA model was firstly proposed by Green and Ampt (1911), which is a physically based mathematical model describing the infiltration process in soils with overlying water. According to the assumption of the model, the soil profile can be divided into a wetting (saturated) region and non-wetting (unsaturated) region during infiltration, the interface between the two regions is termed the wetting front (as shown in Fig. 1). The water is distributed in a rectangular shape in the horizontal soil, the wetting region is the saturated soil layer with the saturated water content θ_s, the non-wetting region consists of the unsaturated (natural) soil layer with initial natural water content θ_i. The infiltration rate f is obtained as

$$f = -k_s \frac{dh}{dz} = -k_s \frac{(h_i - z_f) - h_0}{z_f - 0} = k_s \left(1 + \frac{h_0 - h_i}{z_f}\right) = k_s \left(1 + \frac{h_0 + S_f}{z_f}\right) \tag{1}$$

where S_f (m) is the suction head at the wetting front; h_0 is the constant water head at the ground surface; z_f is the depth of the saturated wetting front (i.e., infiltration depth); h_i is the water head behind the wetting front. Then, the total amount of infiltration I can be evaluated as

$$I = (\theta_s - \theta_i) z_f \tag{2}$$

However, the original GA model has the following significant limitations for describing the infiltration in slopes. (1) Firstly, this model does not consider the effect of rainfall intensity R on the infiltration rate f when simulating the rainfall infiltration, which will overestimate the infiltration amount I and acquire a larger depth of wetting front. (2) Secondly, a sharp wetting front is considered to separate the wetting and natural regions during the rainfall infiltration, hence the classic model does not consider the existing transitional layer in the soil deposit. It has been demonstrated that the soils between the wetting front and the infiltration surface are not fully saturated, therefore at least one transitional layer should be considered between the saturated region and the natural region (Wang et al., 2002; Rao et al., 2006; Ma et al., 2010). If the transitional layer of infiltration process is not considered, the soil weight above the wetting front will be overestimated, resulting in underestimation of the slope stability (i.e., small Fs value). (3) Thirdly, the critical ks is available to separate the infiltration boundary when the variability of k_s is considered (Dou et al., 2014). However, when considering the spatial variability of k_s, it becomes evident that the values of ks vary across different locations within slopes. Consequently, the critical ks is no longer applicable for dividing the infiltration boundary (Jiang et al., 2020).

2.2 Improved Green-Ampt model

To overcome the above shortcomings, an improved GA model is proposed to describe the rainfall infiltration of slopes considering the spatial variability of soil parameters. During rainfall, the most critical issue for the water infiltration into the soil is to determine the infiltration boundary conditions at different times when the ground ponding water forms the

water-runoff with various inclined topography of the slopes. Given that the critical (homogeneous) k_s is not appropriate for the infiltration boundary condition, Jiang et al. (2020) proposed a modified GA model to divide the infiltration boundary by the water ponding time t_p, referred to an improved GA model in their paper. According to the GA infiltration model, the soil infiltration rate f decreases with the increasing cumulative infiltration amount I. For a slope with an inclination angle of α, when the cumulative soil infiltration amount reaches a certain value of I_p (i.e., the cumulative infiltration amount at the surface ponding time t_p), the ground surface begins to accumulate water (Zhang et al., 2014a), at this moment $f = R\cos\alpha = k_s(\cos\alpha + S_f / z_f)$, the cumulative infiltration amount $I_p = (\theta_s - \theta_i)z_f$ can be expressed as:

$$I_p = \frac{(\theta_s - \theta_i)S_f}{\cos\alpha(R/k_s - 1)} \tag{3}$$

where α is the slope angle; R is the rainfall intensity. And the water ponding time t_p is

$$t_p = I_p / (R\cos\alpha) \tag{4}$$

According to the ponding time, the infiltration boundary conditions in the improved GA model can be divided as follows:

1) Unsaturated state

For the rainfall duration $t < t_p$, soil in the infiltration region remains in the unsaturated state, and all the rainwater will infiltrate into the soil. At this point, the corresponding infiltration boundary is controlled by the flow rate, the water content of the soil in the upper region of wetting front is no longer at the saturated water content θ_s. Assuming that

the corresponding water content is θ, the infiltration governing equation can be obtained using Dancy's law:

$$f(0,t) = -\left(k_s \frac{\partial \psi_r(\theta)}{\partial z} - k(\theta) \right) \tag{5}$$

where $f(0, t)$ is the infiltration rate at the soil surface; $\psi_r(\theta)$ is the relative suction of wetting front, which can be expressed as

$$\psi_r(\theta) = \int_{\psi}^{-\infty} \frac{k(\theta)}{k_s} d\psi = \int_{\psi}^{-\infty} \left(\frac{\psi_b}{\psi} \right)^{3\lambda+2} d\psi = \left(\frac{\psi_b}{\psi} \right)^{3\lambda+1} \frac{\psi_b}{3\lambda+1} = S_e^{3+1/\lambda} \frac{\psi_b}{3\lambda+1} \tag{6}$$

where ψ_b is the air entry pressure; λ is the pore distribution index. Then, by integrating in the direction of the wetting front depth:

$$\int_0^{z_f} f(0,t)\,\mathrm{d}z = \int_0^{z_f} k(\theta)\,\mathrm{d}z + k_s \left[\psi_r(\theta) - \psi_r(\theta_i) \right] \tag{7}$$

Since the GA model assumes a rectangular infiltration profile, Eq. (7) can be simplified as follows:

$$f = R\cos\alpha = k(\theta) + \frac{k_s[\psi_r(\theta) - \psi_r(\theta_i)]}{z_f} \tag{8}$$

At last, the depth of wetting front z_f can be mathematically derived from the GA model as follows:

$$z_f = \frac{I}{\theta - \theta_i} = \frac{Rt\cos\alpha}{\theta - \theta_i} \tag{9}$$

By substituting Eq. (9) into Eq. (8), the following nonlinear equation can be obtained

$$f = R\cos\alpha = k(\theta) + \frac{k_s[\psi_r(\theta) - \psi_r(\theta_i)](\theta - \theta_i)}{Rt\cos\alpha} \tag{10}$$

By solving Eq. (10), the distribution of water content θ under different rainfall durations is obtained, which can be incorporated with Eq. (9) to calculate the corresponding depth of wetting front.

2) Saturated state

When the rainfall duration $t \geq t_p$, water ponding starts to form on the slope, and the rainfall intensity exceeds the allowable infiltration rate of the soils. At this moment, the infiltration region on the ground surface is at the fully saturated state, where the infiltration boundary is controlled by the water head (Dou et al., 2014; Jiang et al. 2020). Then, the rainfall infiltration process can be further divided into two stages: (a) the first stage is the free infiltration stage, and (b) the second stage is the water ponding infiltration stage, where the infiltration rate f and cumulative infiltration amount I can be evaluated as (Yao et al., 2019)

$$f(t) = \begin{cases} R\cos\alpha, & t \leq t_p \\ k_s\left(\cos\alpha + S_f / z_f\right), & t > t_p \end{cases} \tag{11}$$

$$I = \int_0^t f(t)dt \tag{12}$$

Integrating Eq. (12) to obtain the cumulative infiltration, the wetting front depth in the infiltration saturation zone can be calculated as

$$z_f = \frac{I}{\theta_s - \theta_i} \tag{13}$$

Therefore, once the k_s and the corresponding rainfall duration t are determined, the corresponding wetting front depth and water content distribution can be obtained from the above two infiltration boundaries. Additionally, the stratified water content is widely admitted in

several experimental studies (Wang et al., 2002; Rao et al., 2006; Ma et al., 2010), which means the soil mass between the wetting front and the infiltration surface is not fully saturated. In this study, the transient zone is considered in the modified model, in which the stratified wetting region above the wetting front is divided into a saturated region and a transient region as shown in Fig. 2(b). It can be observed that the water content distribution includes three parts: saturated layer, transitional layer, and natural layer. The saturated layer depth is z_s, and the transitional layer depth is z_t. Previous studies (e.g., Wang et al., 2003; Peng et al., 2012) have indicated through soil tests that the utilization of an elliptical curve distribution provides a high level of accuracy in characterizing the water content distribution within the transition layer. Hence, in alignment with these research findings, this paper also employs the elliptic curve to describe the water content distribution of the transition layer, as such the distribution of calibrated water content of the soil is obtained as:

$$\begin{cases} \text{Saturated layer}: & \theta(z)=\theta_s, \quad 0\le z\le z_s \\ \text{Transitional layer}: & \theta(z)=\theta_i+(\theta_s-\theta_i)\sqrt{\left[1-(z-z_s)^2/z_t^2\right]}, \quad z_s\le z\le z_h \\ \text{Natural layer}: & \theta(z)=\theta_i, \quad z>z_h \end{cases} \tag{14}$$

where, z_h is the depth of the entire infiltration zone, which can be expressed as

$$z_h = z_s + z_t \tag{15}$$

With effect of the precipitation, the depth of each layer will subsequently change. Through experiments, Peng et al. (2012) found that there is a proportional relationship between the depth of the transitional layer and the depth of the total infiltration zone, and proposed a linear relationship that reads

$$z_t = \eta z_h, \qquad \eta = a z_h + b \tag{16}$$

where η is the ratio of the transitional layer to the depth of the entire infiltration zone; a and b are the coefficients. During the correction process of the transitional layer, the cumulative infiltration will keep constant, $I = I_M$. Cumulative infiltration amount I can be calculated by Eqs. (9) and (12). I_M is the cumulative infiltration after considering the transitional layer, and its value is equal to the sum of the saturated layer infiltration I_s and the transitional layer infiltration I_t. For the saturated layer, the infiltration amount is $I_s = (\theta_s - \theta_i) z_s$; the transitional layer is an elliptic curve distribution, and its infiltration amount is equal to 1/4 of the ellipse area $I_t = 0.25\pi(\theta_s - \theta_i) z_t$. Then, the total cumulative infiltration can be obtained as

$$I = I_M = I_s + I_t = (\theta_s - \theta_i) z_s + 0.25\pi(\theta_s - \theta_i) z_t \tag{17}$$

Based on Eqs. (15) to (17), the depth of the saturated layer z_s and the depth of the transitional layer z_t can be calculated, from which the depth of the infiltration zone and the water content distribution of the entire deposit can be obtained.

3 Stability Analysis of Heterogeneous Slopes

The failure pattern of rainfall-induced slope commonly manifests as shallow landslides that occur parallel to the slope surface (Cho, 2014). The depth of the sliding surface in these cases is generally within the range of 1-3 m (Ray et al., 2010), which is significantly smaller than the overall length of the slope. The relatively small depth of the sliding surface compared to the overall length of the slope allows for the analysis of rainfall-induced slopes as infinite slopes. Therefore, an illustrative infinite slope model is considered to analyze the stability of shallow landslides, as shown in Fig. 3. According to the Mohr-Coulomb failure criterion, the safety

factor, F_S, of the infinite slope based on limit equilibrium analysis (Cho, 2014; Cai et al., 2017) can be calculated from

$$F_S = \frac{\tau_f}{\tau_m} = \frac{c' + [(\sigma_n - u_a) - \sigma_s]\tan\varphi'}{W \sin\alpha \cos\alpha} \tag{18}$$

where τ_f is the shear strength of the soil; τ_m is the shear stress at any point along the potential failure surface; W is the weight of the soil slice; c' and φ' are the effective cohesion and effective friction angle of the soil, respectively; $(\sigma_n - u_a)$ represents the normal force acting on the bottom of the unit soil slice on the wetting front, where σ_n and u_a denote the total stress and the pore air pressure, respectively (Fredlund and Rahardjo, 1993; Ng and Menzies, 2007). According to the literature (Cho, 2014; Dou, et al., 2014; Jiang et al., 2020), u_a = 0 and $\sigma_n = \gamma_t z \cos^2\alpha$, where γ_t is the effective unit weight of the soil, z is the depth of the rupture surface, α is the angle of the infinite slope; σ_s is the suction stress, which can be expressed as

$$\sigma_s = -S_e \psi(\theta) \tag{19}$$

where S_e is the degree of saturation, $S_e = (\theta - \theta_r)/(\theta_s - \theta_r)$, θ_s and θ_r are the saturated water content and residual water content, respectively; $\psi(\theta)$ is the matric suction. During water infiltration, the soil unit weight changes with the change of the water content, the corresponding soil weight W above the rupture surface can be obtained from

$$W = \int_0^z \gamma_t dz \tag{20}$$

where the effective unit weight of the soil, γ_t, is expressed as

$$\gamma_t = \gamma_d + \theta(z)\gamma_w \tag{21}$$

where γ_d and γ_w represent the dry unit weight of soil and unit weight of water, respectively.

Since the focus of this study is to process an improved GA model for the rainfall infiltration analysis of slope. Other soil strength parameters, such as effective cohesion, effective friction angle, are considered as deterministic values due to their minor effects in seepage analysis compared with k_s. However, the variabilities of these parameters can also be incorporated into the proposed analysis framework in future studies. Fig. 4 shows the framework diagram for conducting stability analysis of a heterogeneous slope under rainfall infiltration with the proposed improved GA model. The implementation steps can be summarized as follows:

1) Collect the initial test data on soil parameter values with their mean and standard deviation, and select the autocorrelation function, autocorrelation length, and probability distribution. Determine the depth of the slope (H) and the size of the random field unit (d).
2) Divide the slope into homogeneous soil layers: divide the infinitely long slope into H/d equal-thickness homogeneous soil layers along the vertical direction, and extract the coordinates ($z_{o,i}$) of the centroid of the i-th soil layer, where $i = 1, 2, \cdots, H/d$.
3) Using the statistical information obtained from Step 1, generate N groups of independent standard normal random samples $\boldsymbol{\xi}$ using the Monte Carlo simulation (MCS). Then, simulate N non-Gaussian random fields of k_s with the random samples $\boldsymbol{\xi}$ and the coordinates ($z_{o,i}$) using the Karhunen-Loève (KL) series expansion method. Map these non-Gaussian random fields onto the corresponding soil layers based on the coordinates ($z_{o,i}$).
4) Calculate the water ponding time t_p, and compare it with the rainfall duration t to determine the infiltration boundary conditions, and then the water content distribution of

the slopes considering the transitional layer can be computed from Eqs. (9), (12) and (14) to (17).

5) Calculate the F_S for the rapture surface corresponding to each soil layer bottom and wetting front of the slope using Eq. (18); from the (H/d+1) F_S obtained, select the smallest F_S as the factor of safety of the infinite slope. The corresponding rapture surface is therefore the critical slip surface.

4 Illustrative examples

Considering the illustrative example of an unsaturated infinite slope shown in Fig. 3, the vertical depth, H, of the slope is assumed as 3 m, the slope angle, α, is assumed as 50°. The bottom boundary is an impermeable bedrock, and a rainfall intensity, R, of 5 mm/h is considered. According to the soil-water characteristic curve model from Brook and Corey (1964), the mathematical relationships between the hydraulic conductivity, matric suction and volumetric water content can be expressed as

$$k(\theta) = k_s S_e^{3+2/\lambda} \tag{22}$$

$$\psi(\theta) = \psi_b S_e^{-1/\lambda} \tag{23}$$

The representative values for model parameters used for the analysis in this paper are taken from the literature (Dou et al., 2014) and summarized in Table 1. Additionally, the values for the coefficients a and b related to the depth of transitional layer [as in Eq. (16)] are considered -0.003 and 0.8712, respectively. They are obtained from the test data in Peng et al. (2012).

Four different cases are analyzed to demonstrate the performance of the improved GA model for calculation of water content distribution and associated slope stability under rainfall infiltration. Case I is the most representative example of a homogeneous slope, which provides a baseline scenario in relevant engineering problems. Case II (two-layer soil slopes, the upper

layer with higher permeability and the lower layer with lower permeability) and case III (two-layer soil slopes, the upper layer with lower permeability and the lower layer with higher permeability) are specifically considered to verify the effectiveness of proposed improved GA model when applied to two-layer soil slopes with varying permeability. Case IV is presented for the verification of performance of proposed improved GA model in heterogeneous slopes, considering the spatial variability of k_s. In all cases, for comparison, the computational results obtained from Richards equation and modified GA model (Jiang et al., 2020) are also provided. Noted that the numerical solution from the Richards equation is regarded as the exact solution in this paper.

The Richards equation adopts a one-dimensional flow model to simulate the vertical infiltration process of the slope; the governing equation describing the infiltration of one-dimensional water flow on the slope is expressed as

$$\frac{\partial \theta}{\partial t} = \frac{\partial}{\partial z}\left[k(\theta)\left(\frac{\partial h}{\partial z} - \cos\alpha \right) \right] \tag{24}$$

where θ is the water content, $\theta \in [\theta_r, \theta_s]$; h is the pressure head. The partial differential Eq. (24) can be numerically solved; in this paper, using Hydrua-1D software (Simunek et al., 2013), the pressure head $h(z, t)$ and water content $\theta(z, t)$ values at various depths z under different rainfall durations t can be obtained.

4.1 Case I: Homogeneous slope

Based on the parameter values shown in Table 1, the water content distributions and F_S obtained from Richards equation, the modified GA model and the improved GA model are shown in Fig. 5. It can be seen from Fig. 5(a) that the water content distribution obtained from the modified GA model is quite different from the other two methods. This can be explained by

the assumption in the modified GA model, that only the rectangular infiltration of water is considered and there is no transitional region. In Fig. 5, as rainfall continues, the wetting front gradually moves downwards, resulting in a gradual decrease in the F_S value of the saturated zone with the depth of infiltration increases. However, in the transition layer, due to the soil not being fully saturated, the matrix suction is not completely dissipated. Thus, the F_S of the transition layer initially decreases and then exhibits an increasing trend with depth. After that, within the soil layer, both soil water content and matrix suction are maintained in their initial states. However, as soil depth increases, the self-weight of the soil mass gradually increases, resulting in a decrease of F_S with depth.

Additionally, to determine the critical slip surface under different rainfall durations and identify the landslide triggering factor (i.e., if the critical slip surface of slope occurs in the infiltration area, it can be considered that the slope instability is mainly caused by rainfall infiltration), the F_S of the infiltration zone and the entire slope under the rainfall durations of 20 h, 36 h and 60 h are computed by the three different methods (as shown in Table 2). It should be noticed that the infiltration zone refers to the area where the rainwater permeates into the slope, including the saturated layer and the transitional layer (e.g., the infiltration zone can be defined as 0-1.25 m in Fig. 5(b) for the rainfall duration of 60 h), while the entire slope includes the infiltration zone and the natural zone. According to the results, the Fs of slope decreases with the increase of rainfall duration. Compared with the modified GA model, the improved GA model provides the F_S values that consistently agree with those calculated by the Richards equation. For instance, under the rainfall duration of 60 h, the differences of F_S obtained from the proposed model and the Richards equation is very small (1.22 compared to 1.19). However, the F_S obtained from the modified GA model is relatively smaller, because the modified GA model

assumes the rectangular infiltration of water, which leads to a large water content θ which overestimates the weight W of the soil, and consequently result in small F_S values. The improved GA model considers the objectively existing transitional layer, hence the calculated water content distribution and F_S values are in good agreement with the numerical solution of the Richards equation, which indicates the effectiveness of the proposed model in analyzing the stability of homogeneous slopes under rainfall infiltration.

4.2 Case II: two-layer slope

To further validate the improved GA model, this case considering an upper layer with lower permeability and a lower layer with higher permeability is adopted to conduct the stability analysis under the rainfall infiltration. In this case, the k_s of the upper layer, with 0.5 m thickness, is assumed 3.5 mm/h; the k_s of the lower layer, with 2.5 m thickness, is assumed 3 mm/h. Other parameters of the two layers are kept the same (see Table 1). In Fig. 6, the computed distributions of water content from different methods are quantitatively compared. It shows that the results of the improved GA model are in fairly good agreement with the numerical solution of the Richards equation. Table 3 compares the F_S values of the infiltration zone and the entire slope under the rainfall durations of 20 h, 36 h and 60 h with the three different methods. It shows that the factors of safety from the improved GA model agree well with the numerical solution of the Richards equation. This case also confirms the effectiveness of the proposed model and the significance of considering the transitional layer in the rainfall infiltration problems.

4.3 Case III: two-layer slope

In this case, another two-layer slope model consisting of an upper layer with lower permeability and a lower layer with higher permeability is used to conduct the stability analysis

under rainfall infiltration. The k_s of the upper layer of soil is 3 mm/h, with a thickness of 0.5 m; the k_s of the lower layer is 3.5 mm/h, with a thickness of 2.5 m. Other parameters of the two layers are kept the same. Fig. 7 compares the computed distributions of water content with different methods and Table 4 shows the F_S values of the infiltration zone and the entire slope. Similar with case II, the proposed model produces the results close to the numerical solution of the Richards equation, which further approves the effective performance of the improved GA model.

4.4 Case IV: heterogeneous slope

In reality, the spatial variability of k_s in a soil deposit is widely admitted. In this case, the infinite slope is divided into 60 layers in the vertical direction, where the thickness of each soil layer is d = 0.05 m. The random variable in the soil property is k_s, which is assumed to follow the lognormal distribution with the mean value of 3 mm/h and the standard deviations of 1.5 mm/h (Dou et al., 2014; Jiang et al., 2020). The Gaussian autocorrelation function is utilized for modeling the spatial variability of k_s due to its ability to generate smoother realizations of random fields and requiring fewer KL expansion series (Ma et al., 2022c). The vertical autocorrelation length is taken as 0.5 m. When the number of truncation items of the KL expansion series equals 6, the expectation ratio is 95.67%, which can meet the accuracy requirement of random field discretization (> 95%) (e.g., Laloy et al., 2013; Jiang et al., 2014). By using K-L expansion method, the k_s random field samples are generated.

To conduct a comprehensive analysis of heterogeneous slope stability, MCS analysis is performed with a large number of k_s random field samples. This approach will first calculate the distribution of water content for each MCS sample using the improved GA model. Then it will identify the possible responses and corresponding F_S of the heterogeneous slopes through slope

stability analysis. In total, 1000 samples of spatially varying k_s profiles are generated and analyzed. Each stochastic analysis is conducted with the same boundary conditions that used in the deterministic analysis. Theoretically, a greater number of MCS samples can obtain a higher accuracy of estimated results but it requires a higher computational cost. To check the convergence of the MCS, Fig. 8 shows the statistical mean values μ_{FS} and standard deviations σ_{FS} of the slopes at the rainfall duration of 36 h plotted as functions of the number of the MCS samples using the improved GA model. Based on the convergence criterion, it is shown that the convergence is achieved after about 600 simulations. Therefore, 1000 MCS samples can produce reasonably stable results for this case. Moreover, to compare and validate the solution, in Fig. 8 the results of Richards equation are also presented. It can be observed that the values of μ_{FS} and σ_{FS} evaluated by the proposed improved GA model and Richards equation are consistent with each other.

Fig. 9 presents the calculated water content distributions for 1000 MCS samples using different methods under 36 h rainfall duration. To provide better visualization, Fig. 10 presents and compares the water content distributions of four typical realizations of k_s random field using two methods at the rainfall duration of 36 h. It can be found from Figs. 9 and 10, the water content distributions calculated by the proposed improved GA model are in good agreement with the numerical solution of Richards equation. The results in Figs. 8-10 illustrate the effectiveness of the improved GA model applied in the rainfall infiltration and stability analysis of the heterogeneous slopes.

To further illustrate the effectiveness of proposed improved GA model in analyzing the heterogeneous slopes, a typical example is conducted and described in detail. This typical realization of k_s random field varies over the slope domain is shown in Fig. 11, in which the dark

regions indicating the zones with larger k_s values, while the light parts represent the relatively smaller k_s values. By conducting rainfall infiltration analysis, Fig. 12 shows the distributions of calculated water content using different methods for 8 h, 36 h, and 60 h rainfall durations on this slope. It can be found that under different rainfall durations, the water content distributions calculated by the improved GA model and the numerical solution of the Richards equation are in pretty good agreement, and the F_S of the infiltration zone and the entire slope are almost same (see Table 5).

As shown in Table 5, under the rainfall durations of 8h and 36 h, the F_S values of the entire slope are less than the F_S values of the infiltration zone, indicating that the most critical slip surface is located at the impermeable layer of 3 m. However, under the rainfall durations of 60 h, the F_S of the infiltration zone calculated by the modified GA model is equal to the F_S of the entire slope, indicating a critical slip surface within the infiltration zone which could lead to an erroneous slope instability consideration. The results of both improved GA model and the Richards equation indicate that the critical slip surface is still located at the impermeable layer with 3 m depth. This is because the permeability of the surface soil layer is relatively low, as shown in Fig. 11, and the wetting front progresses slowly. Although the F_S at the wetting front is decreasing continuously, it is always greater than the F_S at the impermeable layer. The comparison shows that the modified GA model may cause incorrect estimation of the slope stability, while the improved GA model can more accurately identify the location of the slope critical slip surface which lead to accurate estimation of the F_S.

5 Conclusions

Considering the transitional layer in the process of rainfall infiltration, this paper proposes an improved GA model for the rainfall infiltration analysis of heterogeneous slopes, which can

effectively determine the wetting front depth and water content distribution. The infinite slope model is taken as an example, the seepage and stability analysis of rainfall infiltration slope is carried out, and the effectiveness of proposed improved GA model is verified by comparing with the numerical results from the Richards equation and the modified GA model. The main conclusions are as follows:

(1) The classic GA model is limited to the rectangular infiltration of rainwater, and does not consider the objectively existing transitional layer, which results in an overestimation of the soil's unit weight in the rainfall infiltration zone, and consequently the calculated F_S of slope is small. This may result in the miscalculation of the slope's stability.

(2) The proposed model takes into account the presence of transitional layer in the infiltration zone, and the calculated water content distribution and F_S show excellent agreement with the numerical solution of the Richards equation, which can better solve the problem of rainfall infiltration in heterogeneous slopes accounting for the spatial variability of k_s.

(3) In case IV, when the rainfall lasts for 60 h, the modified GA model indicate that the critical slip surface is located in the infiltration zone, while both the proposed improved GA model and the numerical method indicate that the critical slip surface of the slope is located at the impermeable layer with a depth of 3 m. Compared with the modified GA model, the proposed improved GA model can better identify the position of the critical slip surface of the heterogeneous slope.

(4) The currently proposed improved GA model is specifically applicable to address the one-dimensional rainfall infiltration problems on heterogeneous slopes under uniform rainfall conditions. Further research could be conducted to incorporate various environmental

factors into rainfall infiltration modeling, including the uneven distribution of the initial water content within slopes, the thickness of slope cover soil, and the random rainfall pattern, etc.

Acknowledgements

The financial support by the National Natural Science Foundation of China Project (Grant: 52222905, 52150610492, 52179103, 42272326 and 41972280) and Jiangxi Provincial Natural Science Foundation (Grant No. 20224ACB204019) are gratefully acknowledged. The third author would like to acknowledge support from Early Career Fellowship of Institute of Advanced Study, University of Warwick.

References

Brooks, R. H., Corey, A. T., 1964. Hydraulic properties of porous media. Hydrology Papers 3, Fort Collins: Colorado State University.

Cai, J. S., Yeh, T. C. J., Yan, E. C., Hao, Y. H., Huang, S. Y., Wen, J. C., 2017. Uncertainty of rainfall-induced landslides considering spatial variability of parameters. Computers and Geotechnics, 87, 149-162.

Chang, Z. L., Huang, F. M., Huang, J. S., Jiang, S. H., Zhou, C. B., Zhu, L., 2021. Experimental study of the failure mode and mechanism of loess fill slopes induced by rainfall. Engineering Geology, 280, 105941.

Chen, L., Young, M. H., 2006. Green-Ampt infiltration model for sloping surfaces. Water

Resources Research, 42, 1-9.

Cho, S., Lee, S.R., 2002. Evaluation of surficial stability for homogeneous slopes considering rainfall characteristics. Journal of Geotechnical and Geoenvironmental Engineering, 128(9), 756-763.

Cho, S. E., 2014. Probabilistic stability analysis of rainfall-induced landslides considering spatial variability of permeability. Engineering Geology, 171, 11-20.

Dolojan, N. L. J., Moriguchi, S., Hashimoto, M., Terada, K., 2021. Mapping method of rainfall-induced landslide hazards by infiltration and slope stability analysis: A case study in Marumori, Miyagi, Japan, during the October 2019 Typhoon Hagibis. Landslides, 2021, 18, 2039-2057.

Dou, H., Han, T., Gong, X., Zhang, J., 2014. Probabilistic slope stability analysis considering the variability of hydraulic conductivity under rainfall infiltration - redistribution conditions. Engineering geology, 183, 1-13.

Fredlund, D. G., Rahardjo, H., 1993. Soil mechanics for unsaturated soils. John Wiley & Sons.

Green, W. H., Ampt, G. A., 1911. Studies on Soil Physics: 1, Flow of air and water through soils. Journal of Agricultural Science, 4(1), 1-24.

He, J., Zhang, L. M., Xiao, T., Wang, H. J., Luo, H. Y., 2023. Prompt Quantitative Risk Assessment for Rain-Induced Landslides. Journal of Geotechnical and Geoenvironmental Engineering, 149(5), 04023023.

Hu, H. J., Li, B. P., Tian, K. L., Ba, Y. D. Cui, Y. J., 2019. Simulation of water movement in unsaturated remolded loves under ponding infiltration and rainfall infiltration. Journal

of Tongji University (Natural Science), 47(11), 1565-1573.

Jiang, S. H., Li, D. Q., Zhang, L. M., Zhou, C. B., 2014. Slope reliability analysis considering spatially variable shear strength parameters using a non-intrusive stochastic finite element method. Engineering Geology, 168, 120-128.

Jiang, S. H., Liu, X., Huang, F. M., Huang, J. S., 2020. Failure mechanism and reliability analysis of soil slopes under rainfall infiltration considering spatial variability of multiple soil parameters. Chinese Journal of Geotechnical Engineering, 42(05), 900-907.

Ko, F. W. Y., Lo, F. L. C., 2018. From landslide susceptibility to landslide frequency: A territory-wide study in Hong Kong. Engineering Geology, 242: 12-22.

Laloy, E., Rogiers, B., Vrugt, J. A., Mallants, D., Diederik, J., 2013. Efficient posterior exploration of a high-dimensional groundwater model from two-stage Markov chain Monte Carlo simulation and polynomial chaos expansion. Water Resources Research, 49(5), 2664-2682.

Li, X. Y., Liu, X., Liu, Y. D., Yang, Z. Y., Zhang, L. M., 2023. Probabilistic slope stability analysis considering the non-stationary and spatially variable permeability under rainfall infiltration-redistribution. Bulletin of Engineering Geology and the Environment, 82(350): 1-16.

Liao, W. W., and Ji, J., 2021. Time-dependent reliability analysis of rainfall-induced shallow landslides considering spatial variability of soil permeability. Computers and

Geotechnics, 129, 103903.

Liu, G., Li, S., Wang, J., 2021. New Green-Ampt model based on fractional derivative and its application in 3D slope stability analysis. Journal of Hydrology, 603, 127084.

Liu X., Liu Y. D., Li X. Y., et al., 2023. Efficient adaptive reliability-based design optimization for geotechnical structures with multiple design parameters. Computers and Geotechnics, 162: 105675.

Ma, G., Hu, X., Yin, Y., Luo, G., Pan, Y., 2018. Failure mechanisms and development of catastrophic rockslides triggered by precipitation and open-pit mining in Emei, Sichuan, China. Landslides, 15, 1401-1414.

Ma, G., Rezania, M. and Nezhad, M.M., 2022a. Stochastic assessment of landslide influence zone by material point method and generalized geotechnical random field theory. International Journal of Geomechanics, 22(4), p.04022002

Ma, G., Rezania, M., Mousavi Nezhad, M. Hu, X., 2022b. Uncertainty quantification of landslide runout motion considering soil interdependent anisotropy and fabric orientation. Landslides, 19(5), 1231-1247.

Ma, G., Rezania, M., and Mousavi Nezhad, M., 2022c. Effects of spatial auto-correlation structure for friction angle on runout distance in heterogeneous sand collapse. Transportation Geotechnics, 33, 10070

Ma, Y., Feng, S., Su, D., Gao, G., Huo, Z., 2010. Modeling water infiltration in a large layered soil column with a modified Green–Ampt model and HYDRUS-1D. Computers and Electronics in Agriculture, 71, S40-S47.

Masoudian, M., Afrapoli, M., Tasalloti, A. M., Marshall, A. M., 2019. A general framework for coupled hydro-mechanical modelling of rainfall-induced instability in unsaturated slopes with multivariate random fields. Computers and Geotechnics, 115, 103162.

Muntohar, A., Liao, H. J., 2009. Analysis of rainfall-induced infinite slope failure during typhoon using a hydrological–geotechnical model. Environmental Geology, 56(6), 1145-1159.

Ng, C. W. W., Shi, Q., 1998. A numerical investigation of the stability of unsaturated soil slopes subjected to transient seepage. Computers and geotechnics, 22(1): 1-28.

Ng, C. W. W., Pang, Y. W., 2000. Influence of stress state on soil-water characteristics and slope stability. Journal of Geotechnical and Geoenvironmental Engineering, 126(2), 157-166.

Ng, C. W. W., Menzies, B., 2007. Advanced unsaturated soil mechanics and engineering. CRC Press.

Ng, C. W. W., Qu, C. X., Ni, J. J., Guo, H. W., 2022. Three-dimensional reliability analysis of unsaturated soil slope considering permeability rotated anisotropy random fields. Computers and Geotechnics, 151: 104944.

Peng, Z. Y., Huang, J. S., Wu, J. W., Guo, H., 2012. Modification of Green-Ampt model based on the stratification hypothesis. Advances in Water Science, 23(1), 59-66.

Phoon, K. K., Kulhawy, F. H., 1999. Characterization of geotechnical variability. Canadian Geotechnical Journal, 4(36), 612-624.

Philip, J. R., 1957. The theory of infiltration: 1. The infiltration equation and its solution. Soil Science, 83(5): 345-358.

Phoon, K. K., Tan, T. S., Chong, P. C., 2007. Numerical simulation of Richards equation in

partially saturated porous media: under-relaxation and mass balance. Geotechnical and Geological Engineering, 25(5), 525-541.

Rao, M. D., Raghuwanshi, N. S., Singh, R., 2006. Development of a physically based 1D-infiltration model for irrigated soils. Agricultural water management, 85(1-2), 165-174.

Ray R. L., Jacobs J. M., De Alba P., 2010 Impacts of unsaturated zone soil moisture and groundwater table on slope instability. Journal of Geotechnical and Geoenvironmental Engineering, 136(10): 1448-1458.

Santoso, A. M., Phoon, K. K., Quek, S., 2011. Effects of soil spatial variability on rainfall-induced landslides. Computers and Structures, 89(11-12), 893-900.

Simunek, J., Van Genuchten, M. T., Sejna, M., 2013. The Hydrus-1D software package for simulating the movement of water, heat, and multiple solutes in variably saturated media, Version 4.16, HYDRUS Software Series 3. Department of Environmental Sciences, University of California Riverside, Riverside, California, USA, p. 340.

Smith, R. E., Corradini, C., Melone, F., 1993. Modeling infiltration for multistorm runoff events. Water Resources Research, 29(1): 133-144.

Wang, W. Y., Wang, Q J., Zhang, J. F., Wang, Z. R., 2002. Soil Hydraulic Properties and Correlation in Qingwangchuan Area of Gansu Province. Journal of Soil and Water Conservation, 16(3), 110-113.

Wang, W. Y., Wang, Z. R., Wang, Q. J., Zhang, J. F., 2003. Improvement and evaluation of the Green-Ampt model in loess soil. Journal of Hydraulic Engineering, 5, 30-34.

Yang, H. Q., Zhang, L. L., Gao, L., Phoon, K. K., Wei, X., 2022. On the importance of landslide management: insights from a 32-year database of landslide consequences and

rainfall in Hong Kong. Engineering Geology, 299, 106578

Yao, W., Li, C., Zhan, H., Zeng, J., 2019. Time-dependent slope stability during intense rainfall with stratified soil water content. Bulletin of Engineering Geology and the Environment, 78, 4805-4819.

Yu, H., Li, C., Zhou, J Q., Chen, W., Zhu, Y., 2022. A semi-analytical model for transient infiltration into inclined soil interlayer considering varying water head and stratified water content. Journal of Hydrology, 614, 128627.

Yuan, J., Papaioannou, I., Straub, D., 2019. Probabilistic failure analysis of infinite slopes under random rainfall processes and spatially variable soil. Georisk: Assessment and Management of Risk for Engineered Systems and Geohazards, 13(1): 20-33.

Zhan, T. L., Ng, C. W. W., 2004. Analytical analysis of rainfall infiltration mechanism in unsaturated soils. International Journal of Geomechanics, 4(4), 273-284.

Zhan, Z. Q., Zhou, C., Liu, C. Q., Ng, C. W. W., 2023. Modelling hydro-mechanical coupled behaviour of unsaturated soil with two-phase two-point material point method. Computers and Geotechnics, 155, 105224.

Zhang, J., Huang, H. W., Zhang, L. M., Zhu, H. H., Shi, B., 2014a. Probabilistic prediction of rainfall-induced slope failure using a mechanics-based model. Engineering Geology, 168: 129-140.

Zhang, J., Han, T. C., Dou, H. Q., Ma, S. G., 2014b. Analysis slope safety based on infiltration model based on stratified assumption. Journal of Central South University (Science and Technology), 45(9): 3211-3218.

Zhang, L. L., Fredlund, D. G., Zhang, L. M., Tang, W. H., 2004. Numerical study of soil conditions under which matric suction can be maintained. Canadian Geotechnical Journal, 41(4), 569-582.

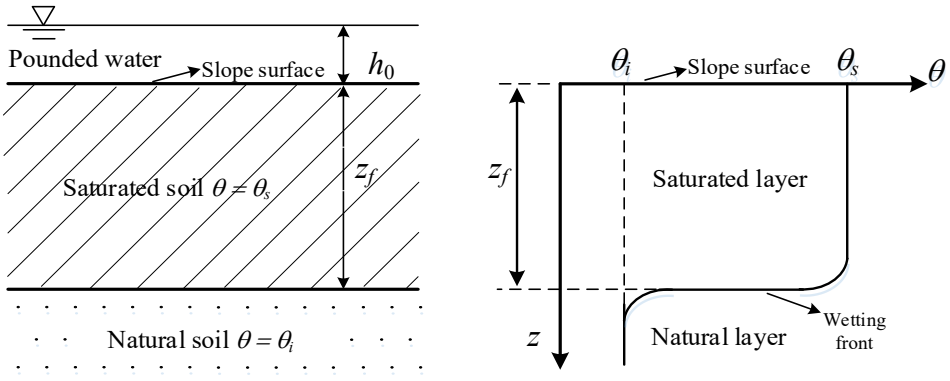

Fig. 1 Water content distribution of the classic GA model.

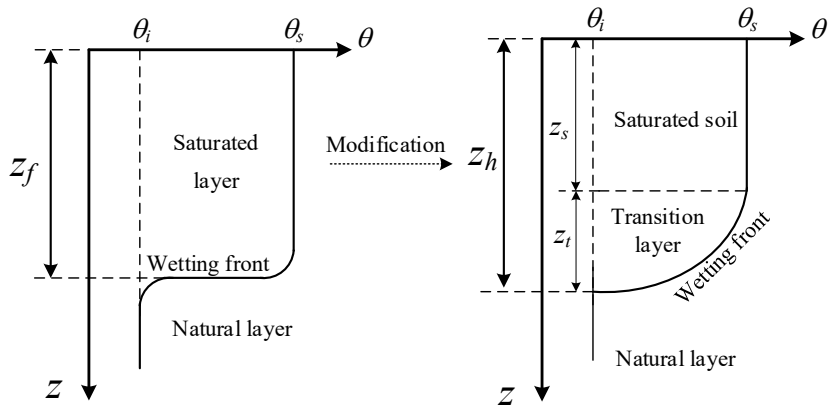

Fig. 2. Water content distributions from (a) Classical GA model, (b) Improved GA model

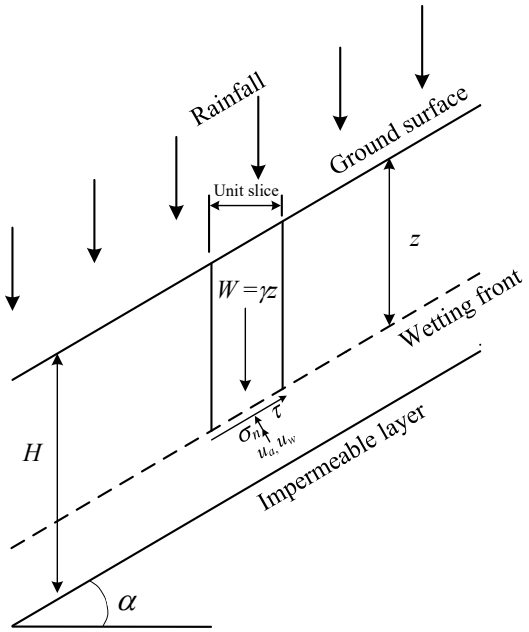

Fig. 3. An infinite slope model.

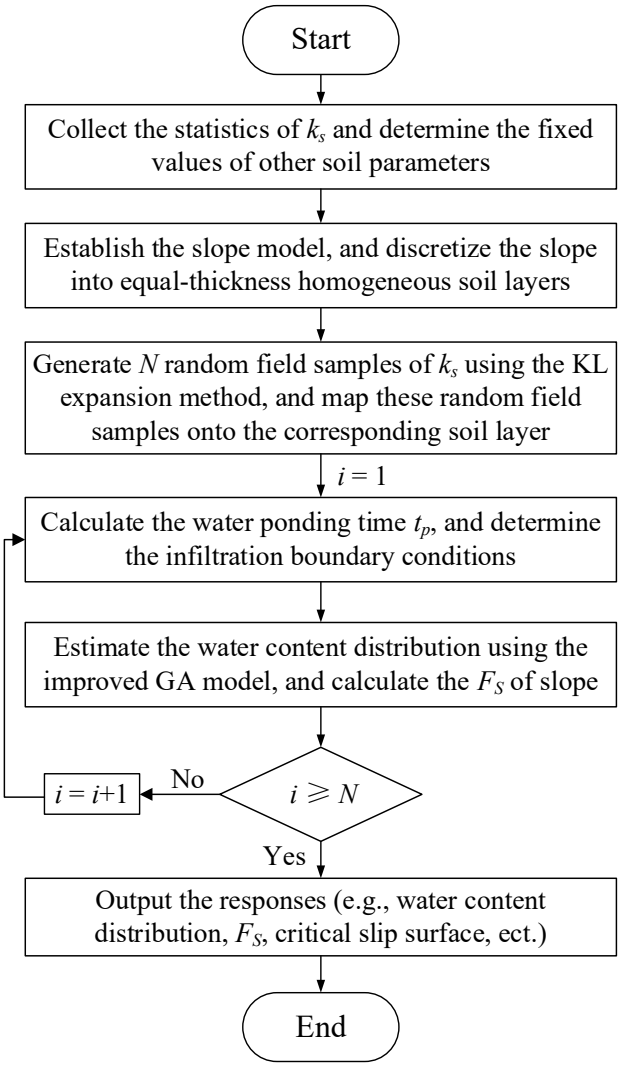

Fig. 4. Framework diagram stability analysis of heterogeneous slopes under rainfall infiltration with the improved GA model.

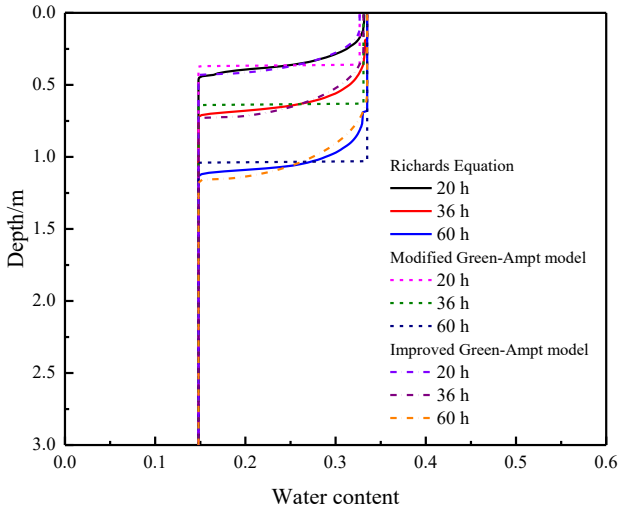

(a) Water content

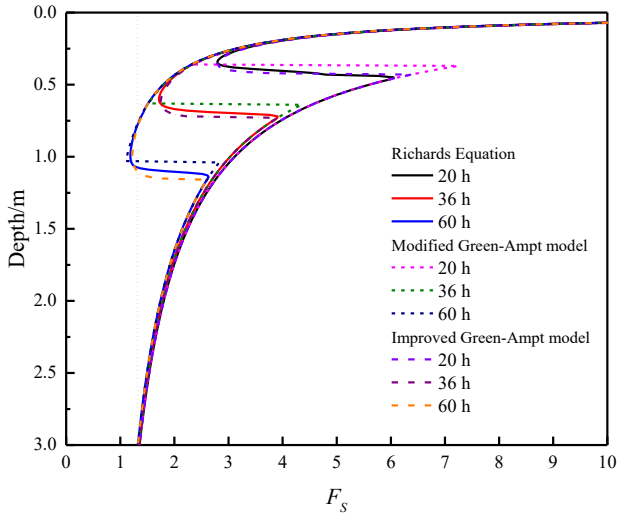

(b) F_S

Fig. 5. Comparison of water content distribution and F_S of slope under different rainfall durations (Case I)

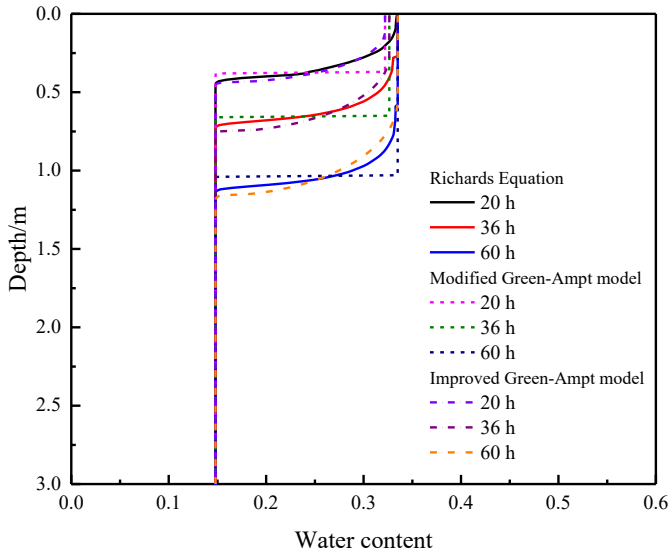

Fig. 6. Comparison of water content distribution of slope under different rainfall durations (Case II)

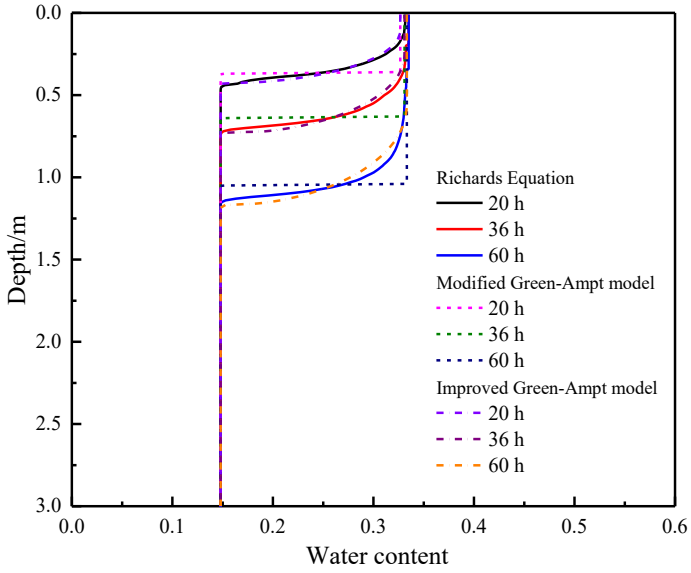

Fig. 7. Comparison of water content distribution of slope under different rainfall durations (Case III)

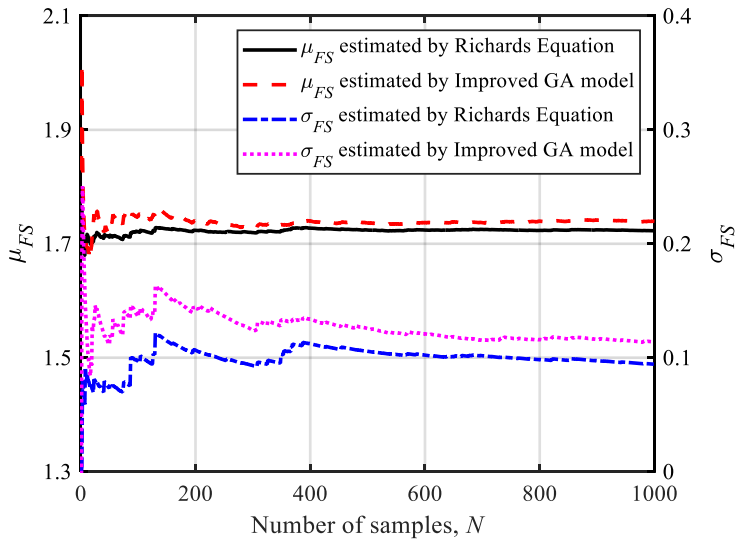

Fig. 8. Variation of statistic of *Fs* of the infiltration zone with number of MCS samples

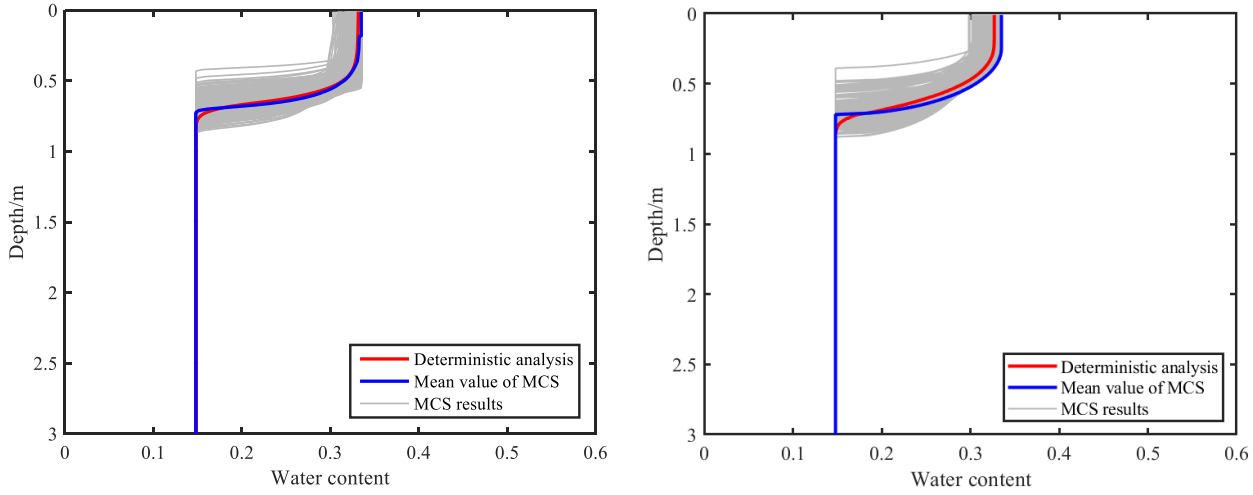

(a) Richards equation (b) Proposed improved GA model

Fig. 9. Water content distribution curves of MCS samples using different method under 36 h rainfall duration.

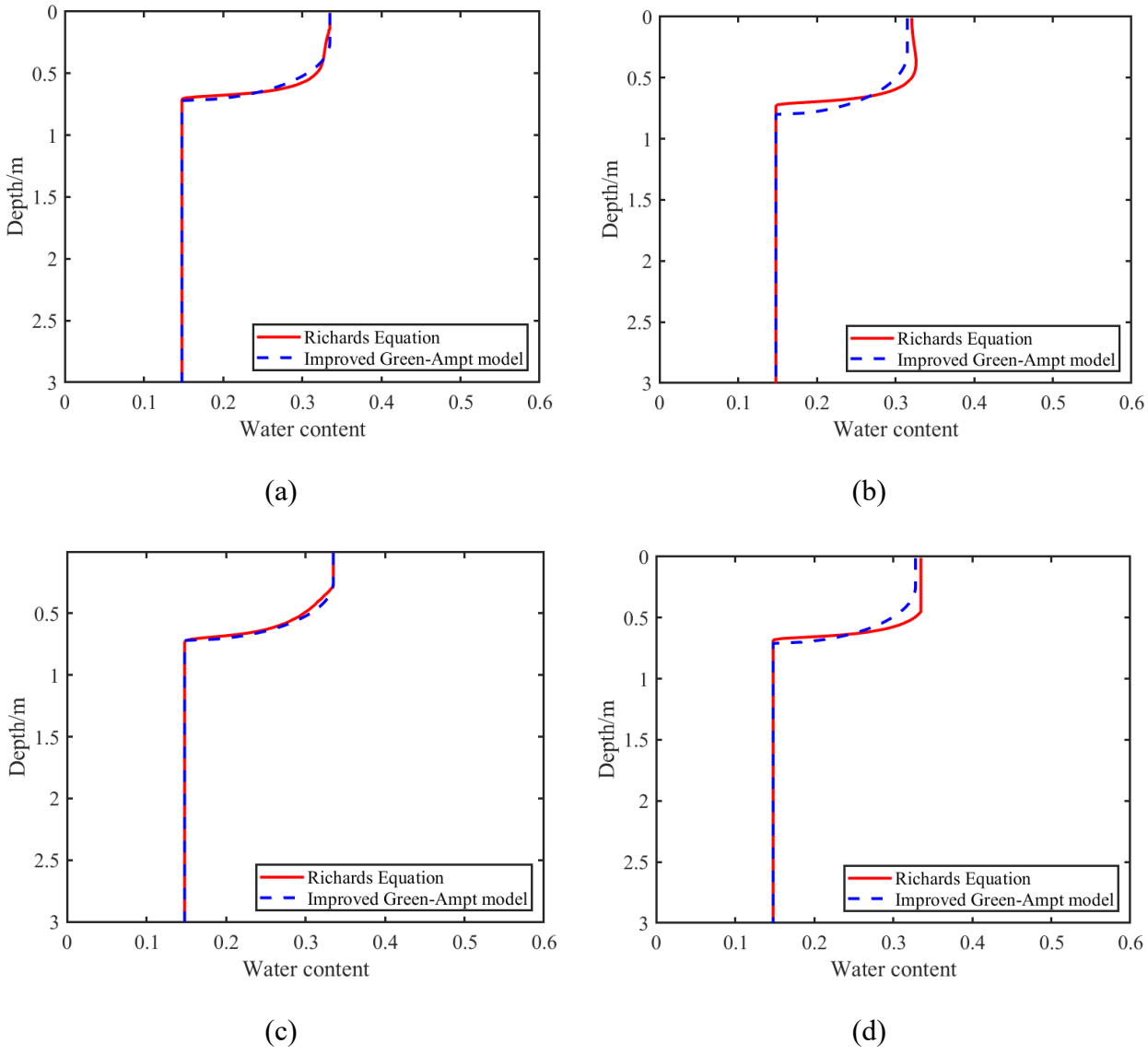

Fig. 10. Comparison of water content distribution curves for four typical realizations at the rainfall duration of 36 h.

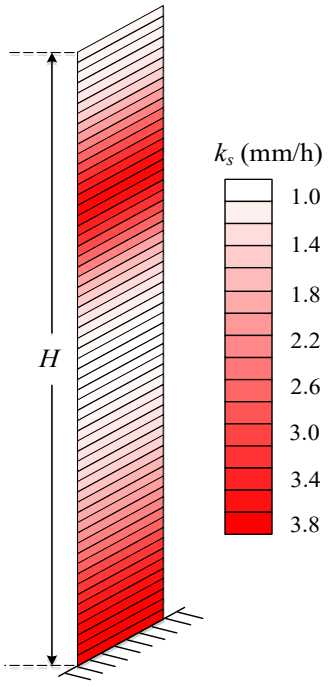

Fig. 11. A typical realization of the random filed of saturated hydraulic conductivity.

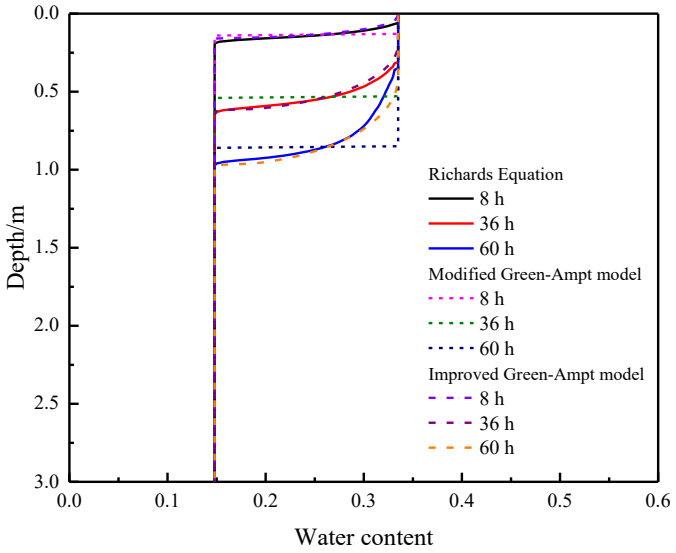

Fig. 12. Comparison of water content distribution of slope under different rainfall durations (Case IV).

Table 1. Physical properties of soil

Parameters	**Unit**	**Value**
Dry density, γ	kN/m^3	16.217
Saturated hydraulic conductivity, k_s	mm/h	3
Effective cohesion, c'	kPa	5
Effective friction angle, φ'	°	28
Saturated water content, θ_s	-	0.335
Residual water content, θ_r	-	0.068
Initial water content, θ_i	-	0.148
Air entry pressure, ψ_b	kPa	2.752
Matric suction of the wetting front, S_f	mm	424.3
Pore distribution index, λ	-	0.319

Table 2. Comparisons of the factor of safety (Case I).

	Duration of rainfall	Solution of Richards equation	Modified GA model	Proposed improved GA model
F_S of infiltration zone	20 h	2.79	2.35	2.78
	36 h	1.72	1.53	1.74
	60 h	1.19	1.10	1.22
F_S of entire slope	20 h	1.36	1.36	1.36
	36 h	1.34	1.34	1.34
	60 h	1.19	1.10	1.22

Table 3. Comparisons of the factor of safety of slope (Case II).

	Duration of rainfall	Solution of Richards equation	Modified GA model	Proposed improved GA model
F_S of infiltration zone	20 h	2.83	2.39	2.81
	36 h	1.71	1.55	1.76
	60 h	1.19	1.10	1.22
F_S of entire slope	20 h	1.36	1.36	1.36
	36 h	1.34	1.34	1.34
	60 h	1.19	1.10	1.22

Table 4. Comparisons of the factor of safety of slope (Case III).

	Duration of rainfall	Solution of Richards equation	Modified GA model	Proposed improved GA model
F_S of infiltration zone	20 h	2.79	2.35	2.78
	36 h	1.72	1.53	1.74
	60 h	1.19	1.10	1.22
F_S of entire slope	20 h	1.36	1.36	1.36
	36 h	1.34	1.34	1.34
	60 h	1.19	1.10	1.22

Table 5. Comparisons of the factor of safety (Case IV)

	Duration of rainfall	Solution of Richards equation	Modified GA model	Proposed improved GA model
F_S of infiltration zone	8 h	6.58	5.62	6.43
	36 h	1.95	1.72	1.98
	60 h	1.40	1.24	1.39
F_S of entire slope	8 h	1.37	1.37	1.37
	36 h	1.35	1.35	1.35
	60 h	1.33	1.24	1.33